A&A 432, 369–379 (2005)
DOI: 10.1051/0004-6361:20041729

Astronomy & Astrophysics

An atomic and molecular database for analysis of submillimetre line observations⋆,⋆⋆

F. L. Schöier[1,3], F. F. S. van der Tak[2], E. F. van Dishoeck[3], and J. H. Black[4]

[1] Stockholm Observatory, AlbaNova, 106 91 Stockholm, Sweden
e-mail: fredrik@astro.su.se
[2] Max-Planck-Institut für Radioastronomie, Auf dem Hügel 69, 53121 Bonn, Germany
[3] Leiden Observatory, PO Box 9513, 2300 RA Leiden, The Netherlands
[4] Onsala Space Observatory, 439 92 Onsala, Sweden

Received 26 July 2004 / Accepted 4 November 2004

Abstract. Atomic and molecular data for the transitions of a number of astrophysically interesting species are summarized, including energy levels, statistical weights, Einstein A-coefficients and collisional rate coefficients. Available collisional data from quantum chemical calculations and experiments are extrapolated to higher energies (up to $E/k \sim 1000$ K). These data, which are made publically available through the WWW at http://www.strw.leidenuniv.nl/~moldata, are essential input for non-LTE line radiative transfer programs. An online version of a computer program for performing statistical equilibrium calculations is also made available as part of the database. Comparisons of calculated emission lines using different sets of collisional rate coefficients are presented. This database should form an important tool in analyzing observations from current and future (sub)millimetre and infrared telescopes.

Key words. astronomical data bases: miscellaneous – atomic data – molecular data – radiative transfer – ISM: atoms – ISM: molecules

1. Introduction

A wide variety of molecules has been detected in space to date ranging from simple molecules like CO to more complex organic molecules like ethers and alcohols. Observations of molecular lines at millimetre and infrared wavelengths, supplemented by careful and detailed modelling, are a powerful tool to investigate the physical and chemical conditions of astrophysical objects (e.g., Genzel 1991; Black 2000). To constrain these conditions, lines with a large range of critical densities and excitation temperatures are needed, since densities typically range from $\sim 10^2$–10^9 cm^{-3} and temperatures from $\sim$10–1000 K in the interstellar and circumstellar environments probed by current and future instrumentation.

In recent years, different molecules have been developed as tracers for different physical and chemical conditions (see van Dishoeck & Hogerheijde 1999, for a review). For example, CO is used as a tracer of the total gas mass whereas readily observed molecules with large dipole moments, such as CS, HCO^+ and HCN constrain the density structure. The wide variety of H_2CO and CH_3OH lines accessible at millimetre and submillimetre wavelengths trace both the temperature and density structure (e.g., Mangum & Wootten 1993). Organic molecules like CH_3OCH_3 and CH_3CN probe the chemical complexity. Deuterated molecules contain a record of the conditions and duration of the cold pre-stellar phase. Si- and S-bearing molecules, in particular SiO and SO_2, probe shocks. Lines of the main species as well as the (generally) optically thin isotopes are needed to determine accurate abundances and line profiles. High frequency lines and vibrationally excited lines are particularly valuable for probing the warm and dense inner parts of the circumstellar envelopes (e.g., Ziurys & Turner 1986; Boonman et al. 2001).

To extract astrophysical parameters, the excitation and radiative transfer of the lines need to be calculated. Indeed, it is becoming increasingly clear that more information – including chemical gradients throughout the source – can be inferred from the data if a good molecular excitation model is available (e.g., Schöier et al. 2002; Maret et al. 2004). The simplest models adopt the "local" approximation, for example in the widely used large velocity gradient (LVG) method. A number of more sophisticated, non-local radiative transfer codes have been developed for the interpretation of molecular line emission (e.g., Bernes 1979; Juvela 1997; Hogerheijde & van der Tak 2000; Ossenkopf et al. 2001; Schöier & Olofsson 2001, see van Zadelhoff et al. 2002, for a review). The application of these codes ranges from protostellar environments to the circumstellar envelopes

⋆ Section 6 and Figs. 3–5 are only available in electronic form at http://www.edpsciences.org

⋆⋆ Datafiles for the atoms and molecules summarized in Tables 2 and 3 are also available in electronic form at the CDS via anonymous ftp to cdsarc.u-strasbg.fr (130.79.128.5) or via http://cdsweb.u-strasbg.fr/cgi-bin/qcat?J/A+A/432/369

of late-type stars. The radiative transfer analysis requires accurate molecular data in the form of energy levels, statistical weights and transition frequencies as well as the spontaneous emission probabilities and collisional rate coefficients. The JPL[1] catalog (Pickett et al. 1998), HITRAN[2] database (Rothman et al. 2003), and the CDMS[3] catalogue (Müller et al. 2001) contain energy levels and transition strengths for a large number of molecular species. Detailed summaries of the theoretical methods and the uncertainties involved in determining collisional rate coefficients are given by Green (1975a), Roueff (1990) and Flower (1990). In this paper, these and other literature data on the rotational transitions of 23 different molecules are summarized and extrapolations of collisional rate coefficients to higher energy levels and temperatures are made. The molecular data files can be found at the webpage `http://www.strw.leidenuniv.nl/~moldata` and is the first effort to systematically collect and present the data in a form easily used in radiative transfer modelling of interstellar regions. The focus is on rotational transitions within the ground vibrational state, but the lowest vibrational levels are included for a few common species where such data are available. Many of the data files presented here were adopted by Schöier et al. (2002) to model the circumstellar environment of the protostar IRAS 16293–2422. In addition, data files for three atomic species are presented. The excitation of atomic fine structure levels plays an important role in cooling of a wide variety of astrophysical objetcs.

An online version of RADEX[4], a statistical equilibrium radiative transfer code using an escape probability formalism, is made available for public use as part of the database. RADEX is comparable to the LVG method and provides a useful tool for rapidly analysing a large set of observational data providing constraints on physical conditions, such as density and kinetic temperature (Jansen et al. 1994; Jansen 1995). RADEX provides an alternative to the widely used rotation temperature diagram method (e.g., Blake et al. 1987) which relies upon the availability of many optically thin emission lines and is useful only in roughly constraining the excitation temperature in addition to the column density. A guide for using the code in practice is provided at the RADEX homepage. RADEX will be presented in more detail in a forthcoming paper (van der Tak et al., in preparation) at which point the source code will be made publically available.

2. Energy levels

In this section the molecular structure is briefly reviewed. This serves merely to provide some basic information needed to properly use the data files. Detailed discussions on molecular (and atomic) structure can be found in, e.g., Townes & Schawlow (1975).

[1] `http://spec.jpl.nasa.gov`
[2] `http://cfa-www.harvard.edu/HITRAN/`
[3] `http://www.cdms.de`
[4] `http://www.strw.leidenuniv.nl/~moldata/radex.html`

2.1. General considerations

The energy levels are obtained from the JPL, HITRAN, and CDMS catalogues. The energy levels and the corresponding line frequencies are thus of spectroscopic quality and may be used for the purpose of line identification, unless stated otherwise.

Generally, we retain only the ground vibrational state and include energy levels up to $E/k \sim 1000$ K. Vibrationally excited levels are usually not well populated in the regions probed by current (sub)millimetre telescopes. Moreover, little is known about collisional rate coefficients for vibrational transitions (e.g., Chandra & Sharma 2001). However, for some specific molecules, e.g. CO and CS, vibrationally excited levels are also included. In the prolongation of this project, data files including vibrational levels will be added for more molecular species.

Molecules with ortho and para versions (or A- and E-type as in the case of e.g. CH_3OH) are treated as separate species.

2.2. Linear molecules

The energy levels for diatomic and linear polyatomic molecules in the $^1\Sigma$ electronic state are quantified, to first order, according to

$$E = BJ(J+1), \tag{1}$$

where B is the rotational constant and related to the moment of inertia I, around axes perpendicular to the internuclear axis, through $B = (2I)^{-1}$. Heavy linear molecules, like HC_3N, have more densely spaced energy levels than diatomic molecules like, e.g., CO. These pure rotational energy levels are classified according to the rotational quantum number J and their statistical weights are

$$g = (2J+1). \tag{2}$$

Note that to obtain state energies of spectroscopic accuracy, Eq. (1) must be augmented with centrifugal distortion ($\propto J^2(J+1)^2$) and higher-order terms. The majority of molecular species presented here have a $^1\Sigma$ electronic ground state, i.e., the sum of the orbital angular momenta of their electrons and the sum of the electron spins are both zero. However, there are some exceptions where either can be non-zero.

For a molecule in a $^2\Sigma$ electronic ground state, e.g., SO and CN, the sum of the electron spins is 1/2. The non-zero spin creates a splitting of the levels due to coupling between the electron spin and the total angular momentum of the molecule. The total angular momentum is quantified according to N and includes the rotation of the molecule. Molecules like, e.g., O_2 have a total electron spin of 1 in a $^3\Sigma$ electronic ground state. Some important molecules such as NO, NS, and OH have a $^2\Pi$ ground state with a total electronic orbital momentum of 1 and total spin of 1/2. Spectroscopically, such molecules show "Λ−Doubling", with $^2\Pi_{1/2}$ and $^2\Pi_{3/2}$ ladders.

The various molecular angular momenta may couple together in many different ways, such as spin-orbit and spin-spin coupling. Ideally, these fall in one of five different classes, known as Hund's coupling cases. In practice, intermediate cases often occur; see Townes & Schawlow (1975) for details.

2.3. Non-linear molecules

The structure of non-linear molecules, such as e.g. H_2CO and CH_3OH, is more complex. Rotation can take place around different axes of inertia, characterized by the rotational constants A, B and C which, in absence of any symmetry, involve different amounts of energy, $A > B > C$. The degree of asymmetry is measured by Ray's parameter

$$\kappa = \frac{2B - A - C}{A - C}, \tag{3}$$

and is -1 for a prolate symmetric top ($B = C$, e.g. CH_3CN) and $+1$ for an oblate symmetric top ($B = A$, e.g. NH_3). Asymmetric rotors such as H_2O have $|\kappa| \ll 1$.

The energy levels of symmetric top molecules, such as NH_3 and CH_3CN, are described by the quantum numbers J and K, where K is the projection of the total angular momentum J on the symmetry axis. For a prolate symmetric top molecule, the energy of a rotational level is given (to first order) by

$$E = BJ(J + 1) + (A - B)K^2. \tag{4}$$

The energy levels for a slightly asymmetric prolate top such as H_2CO can be calculated from

$$E = \frac{B + C}{2} J(J + 1) + \left(A - \frac{B + C}{2}\right) w_{\rm p}, \tag{5}$$

where $w \approx K^2$ with corrections due to the slight asymmetry (Townes & Schawlow 1975, Appendix III).

2.4. Hyperfine splitting

A further complication arises when the nuclear spin couples to the rotation producing what is known as hyperfine splitting. The astrophysically most relevant cases are when the molecule contains a ^{14}N or D nucleus. When the lines are spectroscopically resolved, hyperfine structure provides information on the optical depths, which is otherwise hard to obtain (e.g., Schmid-Burgk et al. 2004).

Hyperfine splitting can be important in line transfer and introduce non-local effects for lines overlapping in frequency, e.g., the $J = 1 \rightarrow 0$ lines of N_2H^+ and HCN. The common assumption is that the hyperfine components each have the same excitation temperature. However, exceptions to this rule ("hyperfine anomalies") have been observed and more detailed treatments developed (Stutzki & Winnewisser 1985; Truong-Bach & Nguyen-Q-Rieu 1989; Lindqvist et al. 2000). Often the splitting between individual hyperfine components is small, producing lines which are separated in frequency by a small amount compared to the line-broadening, so that this splitting can be safely neglected and treated as a single level for the purpose of excitation analysis.

The first release of the database includes hyperfine splitting for some of the most relevant molecules, such as HCN and OH. Future releases will present data files with hyperfine splitting included for additional species.

3. Radiative rates

3.1. General formulae

The radiative rates for dipole transitions from an upper state u to a lower state l can be calculated from

$$A_{ul} = \frac{64\pi^4\nu^3\mu^2}{3c^3h} \frac{\mathcal{S}_{ul}}{g_u}, \tag{6}$$

where μ is the electric dipole moment and $\mathcal{S}$ is the transition strength. The transition strength depends on the complexity of the molecule and is explained below in some detail. Strictly speaking, the dipole moment should be averaged over the vibrational wavefunction(s) of the transition involved ($\mu_{\rm v}$), but in practice often the dipole moment appropriate for the equilibrium geometry is taken ($\mu_{\rm e}$). The electric dipole moments are assumed to be the same for all isotopes of a particular molecule, even though small differences exist for $\mu_{\rm v}$. Because of the ν^3 factor, the resulting Einstein A-values can still differ considerably for isotopes, especially for deuterated species.

For transitions with $\Delta J \pm 1$ in linear molecules, the transition strength is

$$\mathcal{S}_{ul} = g_l \tag{7}$$

whereas for symmetric top molecules, the transition strength from level J, K to $J - 1, K$ is given by

$$\mathcal{S}_{ul} = \frac{J^2 - K^2}{J}. \tag{8}$$

In the general case of asymmetric tops, simple expressions for $\mathcal{S}$ do not exist.

3.2. Dipole moments

Transition strengths are available from the spectroscopic databases mentioned above (JPL, CDMS, HITRAN). There is some inconsistency in the astrophysical literature regarding the choice of values of electric dipole moments, however. This often manifests itself as an apparent bias against results of ab initio theoretical calculations, even when experimental results for transient species are merely estimated or wholly absent. A case in point concerns the pair of ions HCO^+ and HOC^+: the widely cited JPL catalogue offers $\mu = 3.30$ D for HCO^+ and $\mu = 4.0$ D for HOC^+ based on low-level theoretical estimates of Woods et al. (1975) and Gudeman & Woods (1982), respectively, whereas accurate *ab initio* values from Botschwina et al. (1993) give $\mu_0(HCO^+) = 3.93 \pm .01$ D and $\mu_{\rm e}(HOC^+) = 2.74$ D. Ziurys & Apponi (1995) adopted a similar value, $\mu_0(HOC^+) = 2.8$ D, from an ab initio computation of Defrees et al. (1982). Because the inferred column densities scale as $\propto \mu^{-2}$, these discrepancies in dipole moments can result in errors of factors of two in derived abundances.

Table 1 collects values of dipole moments for a (non-exhaustive) sample of molecules of astrophysical interest. Users are encouraged to remain aware of the original literature. Unless otherwise indicated, all entries refer to the electronic and vibrational ground states.

Table 1. Summary of adopted dipole moments[a,b].

Molecule[a]	μ_0 [D]	μ_e [D]	Method	reference
CO	0.110		expt.	1
SO	1.52 ± .02		expt.	2
SO_2	1.633		expt.	3
CS	1.958 ± .005		expt.	4
SiO	3.098		expt.	5
SiS	1.73 ± .06		expt.	6
HCO^+	−3.93 ± .01	−3.90 ± .01	ab initio	7
HOC^+	2.74	2.8	ab initio	8, 9
OCS	0.7152		expt.	10
HC_3N	3.732		expt.	11
HCN	2.985		expt.	12
HNC	3.05 ± .1		expt.	13
HNCO	1.602		expt.	14
c-C_3H_2	3.27 ± .01		expt.	1
CH_3CN	3.922		expt.	15
H_2CO	2.332		expt.	16
N_2H^+		3.4	ab initio	17
HCS^+	1.958		ab initio	18
CH_3OH	0.896		expt.	19
NH_3	1.476 ± .002		expt.	20
H_2O	1.847		expt.	21
SiC_2	2.393 ± .006		expt.	22
HCl	1.109		expt.	23
OH	1.655		expt.	24
H_3O^+	1.44		ab initio	25

[a] Same data are also adopted for isotopes and deuterated species, unless stated in the datafile.
[b] All values are in units of debye (D), where 1 D = 10^{-18} esu cm. When the original source has presented μ in atomic units, a conversion factor of 1 au = ea_0 = 2.54175 D has been applied.
Refs. – (1) Goorvitch (1994); (2) Lovas et al. (1992); (3) Patel et al. (1979); (4) Winnewisser & Cook (1968); (5) Raymonda et al. (1970); (6) Hoeft et al. (1969); (7) Botschwina et al. (1993); (8) Botschwina (1989); (9) Defrees et al. (1982); (10) Muenter (1968); (11) DeLeon & Muenter (1985); (12) Ebenstein & Muenter (1984); (13) Blackman et al. (1976); (14) Hocking et al. (1975); (15) Gadhi et al. (1995); (16) Fabricant et al. (1977); (17) Green et al. (1974); (18) Botschwina & Sebald (1985); (19) Sastry et al. (1981); (20) Cohen & Poynter (1974); (21) From JPL based on Camy-Peyret et al. (1985); (22) Suenram et al. (1989); (23) De Leeuw & Dymanus (1971); (24) Peterson et al. (1984); (25) Botschwina et al. (1984).

For small dipoles, centrifugal corrections to the dipole moment are appreciable. In the case of CO, rotational effects reduce the A-value by 1% for $J = 7$ and by 10% for $J = 22$. The JPL and CDMS catalogues consider this effect and so do our datafiles.

4. Collisional rate coefficients

4.1. General considerations

The rate of collision is equal to

$$C_{ul} = n_{\rm col}\gamma_{ul}, \tag{9}$$

where $n_{\rm col}$ is the number density of the collision partner and γ_{ul} is the downward collisional rate coefficient (in $\rm cm^3\ s^{-1}$). The rate coefficient is the Maxwellian average of the collision cross section, σ,

$$\gamma_{ul} = \left(\frac{8kT}{\pi\mu}\right)^{-1/2}\left(\frac{1}{kT}\right)^2\int \sigma E {\rm e}^{-E/kT}{\rm d}E, \tag{10}$$

where k is the Boltzmann constant, μ is the reduced mass of the system, and E is the center-of-mass collision energy. The upward rates are obtained through detailed balance

$$\gamma_{lu} = \gamma_{ul}\frac{g_u}{g_l}{\rm e}^{-h\nu/kT_{\rm kin}}, \tag{11}$$

where g is a statistical weight.

The collisional rate coefficients γ_{ul} usually pose the largest source of uncertainty of the molecular data input to the radiative transfer analysis (however, see discussion on dipole moments in Sect. 3.2). The dominant collision partner is often H_2 except in photon dominated regions (PDRs) where collisions with electrons and H can become important. The collisional rate coefficients presented here are mainly with H_2 and only in a few cases (in particular the atoms) are collisions with H and electrons also treated. Where available, the data files include collisions with ortho- and para-H_2, e.g., in the case of CO.

If only data for collisions with He are available, a first order correction can be made by assuming H_2 to have the same cross sections. This approximation is strictly only valid for very cold sources, where most H_2 is in the ground $J = 0$ state without angular momentum. Then from Eq. (10) the rate coefficient for collisions between a molecular species X and H_2

$$\gamma_{\rm X-H_2} = \gamma_{\rm X-He}\left(\frac{\mu_{\rm X-He}}{\mu_{\rm X-H_2}}\right)^{1/2}. \tag{12}$$

If the mass of the molecule is much larger than that of He and H_2, the scaling factor is 1.4.

Some molecules of significant interest lack calculated collisional rate coefficients. In these cases the rates for a similar molecule have been adopted and only scaled for the difference in reduced mass following Eq. (12). This procedure works best for O→S substitutions (for example, scaling HCO^+ rates for the case of HCS^+) since such molecules have a similar molecular structure.

For most species, only rate coefficients with He or H_2 $J = 0$ are available. Values with H_2 $J = 1$ can be larger by factors of 2–5 due to supplementary terms in the interaction potential (e.g. Green 1977, H_2O example). This additional uncertainty is often not considered in astrophysical analyses. In the case of CO and H_2O, separate rate coefficients are available for collisions with ortho- and para-H_2. The online version of RADEX weighs these coefficients by the thermal value of the H_2 o/p-ratio at the kinetic temperature. The o/p-ratio is approximated as the $J = 1$ to $J = 0$ population ratio with a maximum of 3.0, which is an overestimate by at most 20% (at $T = 155$ K). In the datafiles available for download the collisional rate coefficients for collisions with ortho-H_2 and para-H_2 are kept separate.

To obtain the collision rate, RADEX simply multiplies the collisional rate coefficients with the H_2 density. To include the

Table 2. Summary of atomic collisional data from the literature.

Atom	T [K]	$E_{\rm max}$ [cm^{-1}]	Collision partner	Ref.
C	10–200	43	H	1
	10–20 000	43	e^-	2
	100–2000	43	H^+	3
	10–150	43	He	4
	10–1200	43	H_2	5
C^+	5–3162	63	H	1
	10–20 000	43 054	e^-	6
	10–250	63	H_2	7
O	50–1000	227	H	1
	50–3000	227	e^-	8
	100–100	227	H^+	9
	20–1500	227	H_2	10

Refs. – (1) Launay & Roueff (1977); (2) Johnson et al. (1987); (3) Roueff & Le Bourlot (1990); (4) Staemmler & Flower (1991); (5) Schröder et al. (1991); (6) Wilson & Bell (2002); (7) Flower & Launay (1977); (8) Bell et al. (1998); (9) Chambaud et al. (1980); (10) Jaquet et al. (1992).

effect of collisions with He, the user must multiply the density by 1.14 (to first order) for a He abundance with respect to H_2 of 20%.

The adopted collisional rate coefficients are presented in Tables 2 and 3 for atomic and molecular species, respectively. For isotopomers the same set of collisional rate coefficients as for the main isotope was adopted, unless otherwise stated. Tables 2 and 3 show the temperature range and maximum energy ($E_{\rm max}$) for which calculations are available. Also, the collision partner is indicated. Only the downward values are given in the data files; the upward rate coefficients are obtained through detailed balance using Eq. (11).

4.2. Accuracy of adopted rate coefficients

Most of the collisional data summarized in Table 2 have been obtained from theoretical calculations, with experimental cross-checks possible for only a few cases. Most experiments reflect the average of many collisional events, with comparisons typically done for relaxation rates and collision-induced pressure line broadening. State-to-state measurements have been possible for only a few systems and they often report relative rather than absolute cross sections. Also, experiments with H_2 are usually done for n-H_2 (i.e., 75% o-H_2 and 25% p-H_2), rather than for H_2 $J = 0$ or 1. Nevertheless, such comparisons between theory and experiment, as well as those between different theoretical methods, have given some indication of the uncertainties in the collisional rate coefficients. Excellent accounts of the methods involved and details on individual systems are given by Green (1975a), Flower (1990) and Roueff (1990); recent developments are reviewed by Roueff et al. (2004). Here only a brief summary is given.

The theoretical determination of collisional rate coefficients consists of two steps: (i) determination of the interaction potential V between the colliding systems; and (ii) calculation of the collision dynamics. Significant progress in the second part has been made in the last decades, aided by the increased computer speed. The most accurate method is the Close-Coupling (CC) method, in which the scattering wave function is expanded into a set of basis functions. This method is exact if an infinite number of basis functions or "channels" is taken into account. In practice a finite number of channels is used, resulting in a set of coupled second-order differential equations. The absolute accuracy of the results can easily be checked by increasing the basis set, and is of order a few % for a given interaction potential. This method works very well for low collision energies and relatively light species, although care should be taken at the lowest energies whether resonances are properly sampled (e.g., Dubernet & Grosjean 2002). However, the method becomes increasingly computationally demanding at high energies and for heavy polyatomic molecules with small splittings between the rotational energy levels resulting in many channels.

The most popular approximate dynamical methods are the Coupled States (CSt) or "centrifugal decoupling" method and the Infinite Order Sudden (IOS) approximation. In the CSt method, the centrifugal potential is assumed to conserve the projection of the angular momentum on the axis perpendicular to the plane of the collision partners. This approximation is often valid at higher energies if the collision is dominated by the repulsive part of the potential. In the IOS approximation, an additional assumption is that the molecule does not rotate during collisions. This may be appropriate for heavy rotors at energies much larger than the rotational energies. From comparisons with the more exact CC results, it is found that absolute uncertainties for the CSt method range from ~10% to a factor of 2, with lesser uncertainties in the relative values. The propensities in the collisions are recovered correctly. In contrast, the IOS method can have uncertainties up to an order of magnitude. Computer programs which include the CC, CSt and IOS options are publically available (see Hutson & Green 1994[5]; Flower et al. 2000[6], Manolopoulos 1986; Alexander & Manolopoulos 1987[7]).

The above quoted ranges of uncertainties assume that the interaction potential is perfectly known. Often, this is not the case and the potential surfaces form the largest source of error in the collisional rates with uncertainties that are difficult to assess. The interaction potential consists of a short-range repulsive part, an intermediate-range interaction part where a weak molecular bond is formed, and a long-range part dominated by electrostatic interaction. The intermediate part is most difficult to determine and requires high-level quantum chemical models. The most accurate method is that of Configuration Interaction (CI), but it can become very costly in computer time. Other methods include Hartree-Fock Self-Consistent-Field (SCF) and perturbation methods, and more recently Density Functional Theory (DFT), but each of these methods has its drawbacks. An old approximate method, the Electron Gas model, is now obsolete, but some dynamics

[5] http://www.giss.nasa.gov/molscat

[6] http://ccp7.dur.ac.uk/molcol.html

[7] http://www.chem.umd.edu/physical/alexander/hibridon

Table 3. Summary of molecular collisional data from the literature and new extrapolated rate coefficients.

Molecule	T [K]	E_{max} [cm^{-1}]	Collision partner	Ref.	Molecule	T [K]	E_{max} [cm^{-1}]	Collision partner	Ref.
CO	5–400	1560	H_2	1	HNCO	30–250	57	He	11*
	100–2000	730	H_2	2	C_3H_2	10–30	82	He	13
	5–2000	3140	H_2	3		30–120	82	He	14
	5–2000	3140	H_2	this work*		30–120	82	H_2	15*
SO	50–350	405	H_2	4*	CH_3CN	20–140	300	H_2	16*
SO_2	25–125	62	He	5	H_2CO	10–300	210	He	17*
	10–375	250	H_2	this work*	N_2H^+	5–40	47	He	18
CS	20–300	310	H_2	6		10–2000	1440	H_2	this work*
	20–2000	1340	H_2	this work*	HCS^+	10–60	64	He	19
SiO	20–300	275	H_2	6		10–2000	660	H_2	this work*
	20–2000	1185	H_2	this work*	CH_3OH	5–200	360	H_2	20*
SiS	20–2000	500	H_2	this work*		5–200	360	He	21, 22
HCO^+	10–400	565	H_2	7	NH_3	15–300	420	H_2	23*
	10–2000	1380	H_2	this work*	H_2O	20–2000	1395	He	24*
OCS	10–150	165	He	8		5–20	140	H_2	25, 26
	10–100	32	H_2	9*		20–140	140	H_2	27
HC_3N	10–80	64	He	9*	HDO	50–500	385	He	28*
HCN	5–100	83	He	10	SiC_2	25–125	50	H_2	15*
	100–1200	1284	He	11	OH	15–300	610	H_2	29*
	10–30	30	He	12	HCl	10–300	580	He	30*
	5–1200	1280	H_2	this work*	H_3O^+	100–100	260	H_2	31*
HNC	5–1200	1310	H_2	this work*					

* Datafile adopted in the online version of RADEX

Refs. – (1) Flower (2001a); (2) Schinke et al. (1985); (3) Larsson et al. (2002); (4) Green (1994); (5) Green (1995); (6) Turner et al. (1992); (7) Flower (1999); (8) Flower (2001b); (9) Green & Chapman (1978); (10) Green & Thaddeus (1974); (11) Green (unpublished data); (12) Monteiro & Stutzki (1986); (13) Avery & Green (1989); (14) Green et al. (1987); (15) Chandra & Kegel (2000); (16) Green (1986); (17) Green (1991); (18) Green (1975b); (19) Monteiro (1984); (20) Pottage et al. (2004); (21) Pottage et al. (2001); (22) Pottage et al. (2002); (23) Danby et al. (1988); (24) Green et al. (1993); (25) Dubernet & Grosjean (2002); (26) Grosjean et al. (2003); (27) Phillips et al. (1996); (28) Green (1989); (29) Offer et al. (1994); (30) Neufeld & Green (1994); (31) Phillips et al. (1992).

calculations for astrophysical systems still use these potentials (e.g., CS-H_2, Turner et al. 1992).

The following selected examples serve to illustrate the range of absolute errors in the adopted collisional rate coefficients. It should be noted that relative values often have less uncertainty and that these are most relevant for astrophysical applications: small absolute errors can often be compensated by small adjustments in the abundance of the species.

4.2.1. CO–H_2

Early calculations by Green & Thaddeus (1976), Schinke et al. (1985) and Flower & Launay (1985) illustrate the sensitivity of the results to different potential energy surfaces. Absolute differences in individual collisional rate coefficients range from a few % up to 40%, with the relative values usually having less scatter. Comparison of computed cross sections using a new CO–H_2 potential by Jankowski & Szalewicz (1998) with pressure broadening and scattering experiments by Mengel et al. (2000) suggests an overall average absolute accuracy of better than 10% at $T \geq 30$ K, but somewhat less good at the lowest temperatures where the deviations can increase to 30–50%. No information is available on the accuracy of the larger ΔJ transitions (e.g., $\Delta J > 10$), which become important at high temperatures such as found in dense shocks. The same potential surface has been used in the latest set of rate coefficients given by Flower (2001a) which are adopted here.

The following simple test problem illustrates the consequences of using different sets of collisional rate coefficients. Line intensities were calculated for the lowest 5 rotational transitions of CO for a molecular cloud of constant temperature and density using RADEX. The model has a temperature of 10 K, H_2 density of 1×10^3 cm^{-3} and a total CO column density of 3×10^{16} cm^{-2} over a line width (full-width at half-maximum) of 1 km s^{-1}. All lines are out of thermal equilibrium and the three lowest rotational transitions are optically thick. As is shown in Fig. 1, differences of up to ±150% are found, especially for collisions with para-H_2 compared with ortho-H_2.

4.2.2. H_2CO–H_2

The H_2CO–H_2 rate coefficients given in our database are obtained from Green (1991), who calculated values for the H_2CO–He system using a very old potential energy surface by Garrison et al. (1975) based on SCF and limited CI calculations. These rate coefficients and the adopted surface have recently been tested against pressure broadening and time-resolved double-resonance studies for three low-lying transitions (Mengel & De Lucia 2000). Satisfactory agreement is

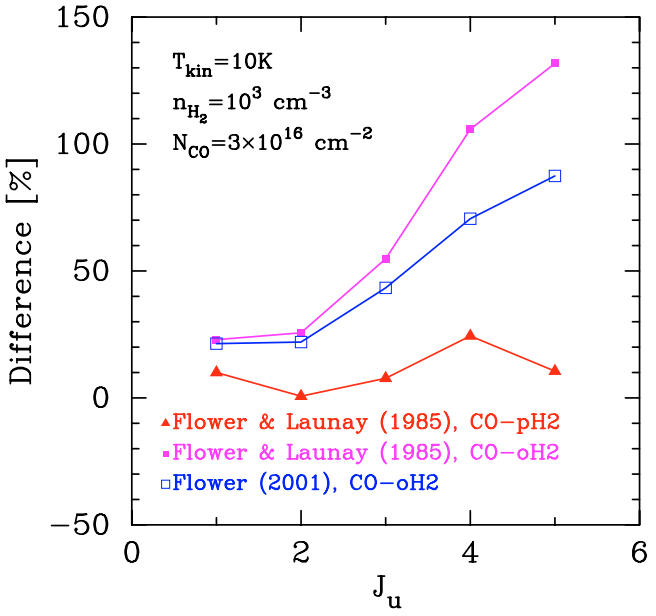

Fig. 1. Predicted CO line intensities, using different sets of calculated collisional rate coefficients, for an isothermal homogeneous sphere with a kinetic temperature 10 K, a H_2 density of 10^3 cm^{-3} and a CO column density of 3×10^{16} cm^{-2}. The line intensities are shown in relation to the values obtained using the CO-pH_2 rate coefficients from Flower (2001a). The upper rotational quantum number J_u is indicated on the x-axis. The rotational transitions are out of thermal equilibrium and, for transitions below $J = 4 \rightarrow 3$, optically thick.

found for the H_2CO–He system, with differences in cross sections ranging from a few % up to 20%. The deviations are largest at the lowest temperatures, <10 K, as was also found for CO–H_2. For H_2 as the collision partner, the cross sections are found to be up to a factor of two higher, significantly more than the value of 1.4 expected from the difference in masses, illustrating that simple scaling from He collisions may introduce errors up to 50%.

4.2.3. OH–H_2

One of the computationally most challenging systems is OH–H_2, since OH is an open shell molecule with a $^2\Pi$ ground state so that two potential surfaces and hyperfine splitting are involved. Results for collisions with both o-H_2 and p-H_2 are presented by Offer & van Dishoeck (1992) using an old potential surface based on SCF calculations (Kochanski & Flower 1981), and by Offer et al. (1994) using a new surface computed using CI (Offer & van Hemert 1993). The differences due to the potential energy surface range from 10% to more than an order of magnitude for individual rate coefficients. Comparison with state-to-state experimental cross sections with both n-H_2 and p-H_2 at one specific energy gives surprisingly good agreement, usually within 50% but with occasional excursions up to an order of magnitude (Schreel & ter Meulen 1996). Moreover, all the propensities for individual hyperfine transitions are well reproduced.

4.3. Adopted collisional rate coefficients

Below follows a summary of the collisional rate coefficients adopted in the first release of the database. Molecules for which only one set of calculated collisional rate coefficients is available and where no extrapolation was performed are not described further here. The principle method for extrapolating the downward collisional rate coefficients ($\Delta J = J_u \rightarrow J_l$, $J_u > J_l$) in temperature in the case of a linear molecule is (de Jong et al. 1975; Bieging et al. 1998)

$$\gamma_{ul} = a(\Delta J) y \exp\left[-b(\Delta J) y^{1/4}\right] \times \exp\left[-c(\Delta J) y^{1/2}\right], \qquad (13)$$

where $y = \Delta E_{ul}/kT$ and the three parameters a, b, and c are determined by least-squares fits to the initial set of rate coefficients for each ΔJ. This reproduces most of the calculated rate coefficients to within 50% and typically within 20%. For more details on the extrapolation scheme, including extrapolation in energy levels, see Sect. 6 (only available in the online version of this journal).

When the specified kinetic temperature falls outside the region where collisional rate coefficients are available, i.e. from $T_{\rm low}$ to $T_{\rm high}$, RADEX makes no further extrapolation and assumes the downward rate coefficients at $T_{\rm low}$ and $T_{\rm high}$, respectively.

4.3.1. CO

For CO the collisional rate coefficients calculated by Flower (2001a) have been adopted as a starting point. These computations cover temperatures in the range from 5 K up to 400 K and include rotational levels up to $J = 29$ and $J = 20$ for collisions with para-H_2 and ortho-H_2, respectively. Both sets of rate coefficients were then extrapolated to include energy levels up to $J = 40$ (using Eq. (18)) and temperatures up to 2000 K (using Eq. (13)), as described in Sect. 6.1. In the datafile available for download, the collisional rate coefficients for collisions with ortho-H_2 and para-H_2 are kept separate. However, in RADEX they are weighted together as described in Sect. 4.1.

Figure 2 shows the extrapolation of CO collisional deexcitation rate coefficients for collisions with para-H_2. It is clear that extrapolated rate coefficients are uncertain and depend on both the original data set from which the extrapolation is made and the method adopted. However, the extrapolated values typically agree within 50% in the case of CO. The largest discrepancies, up to an order of magnitude, naturally arise in the region where extrapolation in both temperature and energy levels are performed. Thus, in the parts of parameter space where extrapolated rates are being used to infer physical conditions, care should be taken as to any astrophysical conclusions drawn from the modeling.

4.3.2. CS

For CS the rate coefficients calculated by Turner et al. (1992) have been adopted as a starting point. These values have been computed for temperatures in the range 20–300 K and include rotational levels up to $J = 20$ for collisions with H_2. This set

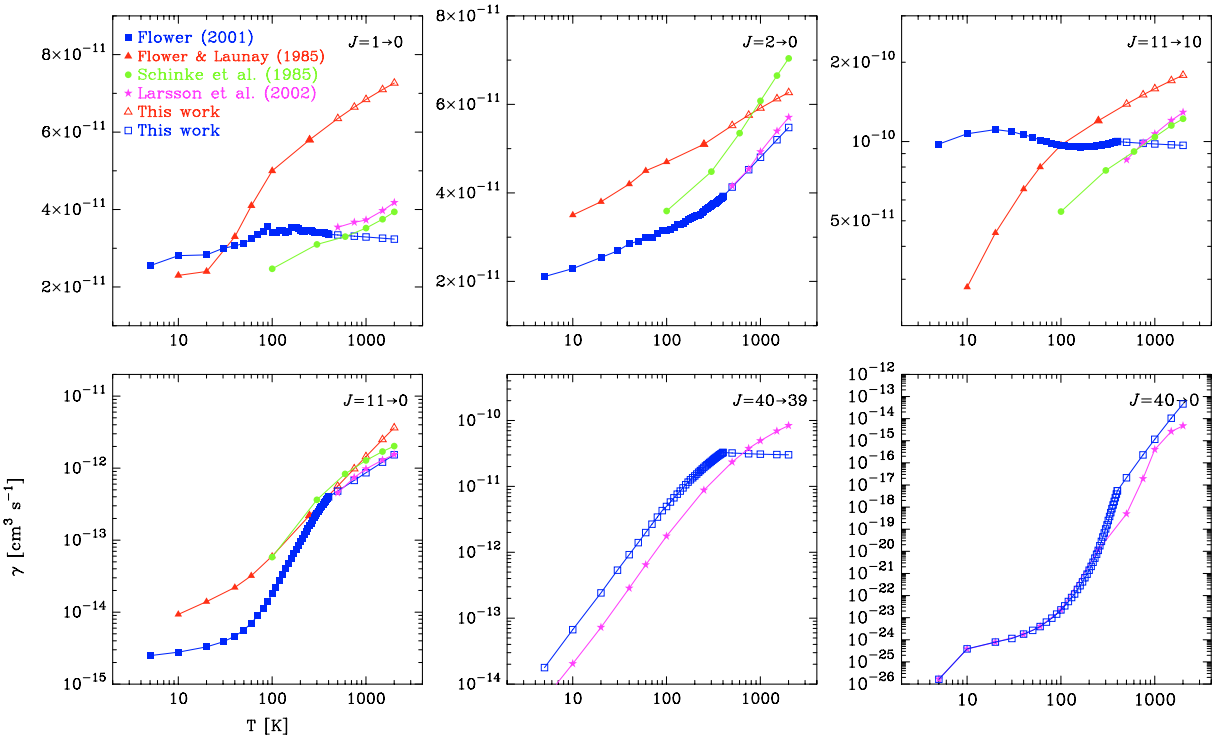

Fig. 2. Calculated and extrapolated collisional de-excitation rate coefficients for CO in collisions with para-H_2. Open triangles indicate extrapolation in temperature to the rate coefficients of Flower & Launay (1985) (filled triangles). Open squares show the extrapolation to higher temperatures and energy levels of the recent rate coefficients calculated by Flower (2001a) (filled squares). For comparison the rate coefficients presented by Schinke et al. (1985) (filled circles) and the extrapolation performed by Larsson et al. (2002) (filled stars) are shown.

was then extrapolated to include energy levels up to $J = 40$ (using Eq. (18)) and temperatures up to 2000 K (using Eq. (13)), as described in Sect. 6.1. No extrapolation to temperatures lower than 20 K was attempted.

4.3.3. SiO

For SiO the rate coefficients calculated by Turner et al. (1992) have been adopted, computed for temperatures in the range 20−300 K and including rotational levels up to $J = 20$ for collisions with H_2. This set was then extrapolated to include energy levels up to $J = 50$ (using Eq. (18)) and temperatures up to 2000 K (using Eq. (13)), as described in Sect. 6.1. No extrapolation to temperatures lower than 20 K was attempted.

4.3.4. SiS

No calculated rate coefficients are available for SiS. Instead, the same set of collisional rate coefficients as for SiO has been adopted.

4.3.5. HCO^+

The rate coefficients for HCO^+ in collisions with H_2 have been calculated by Flower (1999) for temperatures in the range 10−400 K and rotational levels up to $J = 20$. This set of rate coefficients was then extrapolated to include energy levels up to $J = 30$ (using Eq. (18)) and temperatures up to 2000 K (using Eq. (13)), as described in Sect. 6.1.

4.3.6. HC_3N

The rate coefficients for HC_3N in collisions with He have been calculated by Green & Chapman (1978) for temperatures in the range 10−80 K and rotational levels up to $J = 20$. This set of rate coefficients was then extrapolated to include energy levels up to $J = 50$ (using Eq. (18)) and temperatures up to 2000 K (using Eq. (13)), as described in Sect. 6.1. The rate coefficients were then scaled by 1.39 to represent collisions with H_2 instead of He.

4.3.7. HCN

The rate coefficients for HCN in collisions with He have been calculated by Green & Thaddeus (1974) for temperatures in the range 5−100 K and rotational levels up to $J = 7$. This work has subsequently been extended by S. Green (unpublished data) to include rotational levels up to $J = 29$ and temperatures from 100−1200 K. Extrapolation of the rate coefficients to include energy levels up to $J = 29$ for temperatures below 100 K (using Eq. (18)), as described in Sect. 6.1, has been made. The rate coefficients were subsequently scaled by 1.37 to represent collisions with H_2 instead of He. The collisional rate coefficients between various hyperfine levels have been calculated by Monteiro & Stutzki (1986) for the lowest ($J \leq 4$) rotational levels and temperatures from 10−30 K in collisions with He. A datafile based on these collisional rate coefficients is also made available separately.

4.3.8. HNC

No calculated rate coefficients are available for HNC. Instead, the same set of collisional rate coefficients as for HCN has been adopted.

4.3.9. N_2H^+

The rate coefficients for N_2H^+ in collisions with He atoms have been calculated by Green (1975b) for temperatures in the range 5−40 K and rotational levels up to $J = 6$. Given the limited range in temperature and energy levels, we have instead adopted the same rate coefficients as for HCO^+. This is motivated by the discussion in Monteiro (1984) where the rate coefficients for these two species in collisions with He are found to be very similar, typically within 10%.

4.3.10. HCS^+

The rate coefficients for HCS^+ in collisions with He atoms have been calculated by Monteiro (1984) for temperatures in the range 10−60 K and rotational levels up to $J = 10$. This set of rate coefficients was then extrapolated to include energy levels up to $J = 23$ (using Eq. (18)) and temperatures up to 1000 K (using Eq. (13)), as described in Sect. 6.1. The rate coefficients were subsequently scaled by 1.38 to represent collisions with H_2 instead of He.

4.3.11. H_2O

In RADEX the rate coefficients for H_2O in collisions with He calculated by Green et al. (1993) are used as default. The rates were computed for temperatures in the range from 20 to 2000 K including energy levels up to about 1400 cm^{-1}. These rate coefficients were subsequently scaled by 1.35 to represent collisions with H_2 instead of He. In addition, a datafile containing the recent rate coefficients for H_2O in collisions with p-H_2 (Grosjean et al. 2003) and o-H_2 (Dubernet & Grosjean 2002) calculated for low temperatures (5−20 K) has been constructed. In the datafiles available for download, the rate coefficients for collisions with ortho-H_2 and para-H_2 are kept separate. However, in RADEX they are weighted together as described in Sect. 5.1.

4.3.12. SO_2

For non-linear molecules there are no simple scaling relations such as Eq. (13). In Sect. 6.2 (only available in the online version of this paper) the procedure adopted to extrapolate rate coefficients for SO_2 is presented. As starting point the calculated rate coefficients for SO_2 in collisions with He calculated by Green (1995) were used. These rates were computed for temperatures in the range from 25 to 125 K including energy levels up to about 62 cm^{-1}. Extrapolation was made to include energy levels up to 250 cm^{-1} and temperatures in the range from 10 to 375 K. The rate coefficients were subsequently scaled by 1.4 to represent collisions with H_2 instead of He.

5. Summary

A compilation of atomic and molecular data in a homogeneous format relevant for radiative transfer modelling is presented. The data files are made available through the WWW and include energy levels, statistical weights, Einstein A-coefficients and collisional rate coefficients. Extrapolation of collisional rate coefficients are generally needed and different schemes for this are reviewed.

In addition to the atomic and molecular database, an online version of a computer code for performing statistical equilibrium calculations is made available for use through the WWW. The program, named RADEX, is an alternative to the widely used rotation diagram method and has the advantage of supplying the user with physical parameters such as density and temperature.

Databases such as these depend heavily on the efforts by the chemical physics community to provide the relevant atomic and molecular data. We strongly encourage further efforts in this direction, so that the current extrapolations of collisional rate coefficients can be replaced by actual calculations in future releases.

Acknowledgements. The authors are grateful to D. J. Jansen and F. P. Helmich for contributions to the data files and programs. B. Larsson is thanked for providing his collisional rate coefficients for CO. The referee A. Markwick is thanked for a constructive report that helped improve both the paper as well as the online database. This research was supported by the Netherlands Organization for Scientific Research (NWO) grant 614.041.004 and a NWO Spinoza grant. F.L.S. and J.H.B. further acknowledge financial support from the Swedish Research Council.

References

Albrecht, M. A. 1983, A&A, 127, 409
Alexander, M. H., & Manolopoulos, D. E. 1987, J. Chem. Phys., 86, 2044
Avery, L. W., & Green, S. 1989, ApJ, 337, 306
Bell, K. L., Berrington, K. A., & Thomas, M. R. J. 1998, MNRAS, 293, L83
Bernes, C. 1979, A&A, 73, 67
Bieging, J. H., Knee, L. B. G., Latter, W. B., & Olofsson, H. 1998, A&A, 339, 811
Black, J. H. 2000, in Astrochemistry: From Molecular Clouds to Planetary Systems, ed. Y. C. Minh, & E. F. van Dishoeck, (ASP), 197, 81
Blackman, G. L., Brown, R. D., Godrey, P. D., & Gunn, H. I. 1976, Nature, 261, 395
Blake, G. A., Sutton, E. C., Masson, C. R., & Phillips, T. G. 1987, ApJ, 315, 621
Boonman, A. M. S., Stark, R., van der Tak, F. F. S., et al. 2001, ApJ, 553, L63
Botschwina, P. 1989, in Ion and Cluster Spectroscopy and Structure, ed. J. P. Maier (New York: Elsevier), 59
Botschwina, P., Horn, M., Flügge, J., & Seeger, S. 1993, J. Chem. Soc. Faraday Transfer, 89, 2219
Botschwina, P., Rosmus, P., & Reinsch, E. A. 1984, Chem. Phys. Lett., 102, 299

Botschwina, P., & Sebald, P. 1985, J. Mol. Spectrosc., 110, 1
Camy-Peyret, C., Flaud, J.-M., Mandin, J.-Y., et al. 1985, J. Chim. Phys., 113, 208
Chambaud, G., Levy, B., Millie, P., et al. 1980, J. Phys. B At. Mol. Phys., 13, 4205
Chandra, S., & Kegel, W. H. 2000, A&AS, 142, 113
Chandra, S., & Sharma, A. K. 2001, A&A, 376, 356
Cohen, E. A., & Poynter, R. L. 1974, J. Mol. Spectrosc., 53, 131
Danby, G., Flower, D. R., Valiron, P., Schilke, P., & Walmsley, C. M. 1988, MNRAS, 235, 229
de Jong, T., Dalgarno, A., & Chu, S.-I. 1975, ApJ, 199, 69
De Leeuw, F. H., & Dymanus, A. 1971, 26th Symposium on Molecular Spectroscopy, Columbus, Ohio
Defrees, D. J., Loew, G. H., & McLean, A. D. 1982, ApJ, 257, 376
DeLeon, R. L., & Muenter, J. S. 1985, J. Chem. Phys., 82, 1702
DePristo, A. E., Augustin, S. D., Ramaswamy, R., & Rabitz, H. 1979, J. Chem. Phys., 71, 850
Dubernet, M.-L., & Grosjean, A. 2002, A&A, 390, 793
Ebenstein, W. L., & Muenter, J. S. 1984, J. Chem. Phys., 80, 3989
Fabricant, B., Krieger, D., & Muenter, J. S. 1977, J. Chem. Phys., 67, 1576
Flower, D. 1990, Molecular collisions in the interstellar medium, Cambridge Astrophysics Series (Cambridge: University Press)
Flower, D. R. 1999, MNRAS, 305, 651
Flower, D. R. 2001a, J. Phys. B, 34, 2731
Flower, D. R. 2001b, MNRAS, 328, 147
Flower, D. R., Bourhis, G., & Launay, J.-M. 2000, Comp. Phys. Comm., 131, 187
Flower, D. R., & Launay, J. M. 1977, J. Phys. B, 10, 3673
Flower, D. R., & Launay, J. M. 1985, MNRAS, 214, 271
Gadhi, J., Lahrouni, A., Legrand, J., & Demaison, J. 1995, J. Chem. Phys., 92, 1984
Garrison, B. J., Lester, W. A., & Schaefer, H. F. 1975, J. Chem. Phys., 63, 1449
Genzel, R. 1991, in NATO ASIC Proc. 342: The Physics of Star Formation and Early Stellar Evolution, 155
Goldflam, R., Kouri, D. J., & Green, S. 1977, J. Chem. Phys., 67, 4149
Goorvitch, D. 1994, ApJS, 95, 535
Green, S. 1975a, in Atomic and molecular physics and the interstellar matter (Amsterdam: North-Holland Publishing Co.), 83
Green, S. 1975b, ApJ, 201, 366
Green, S. 1986, ApJ, 309, 331
Green, S. 1989, ApJS, 70, 813
Green, S. 1991, ApJS, 76, 979
Green, S. 1994, ApJ, 434, 188
Green, S. 1995, ApJS, 100, 213
Green, S., & Chapman, S. 1978, ApJS, 37, 169
Green, S., Defrees, D. J., & McLean, A. D. 1987, ApJS, 65, 175
Green, S., Maluendes, S., & McLean, A. D. 1993, ApJS, 85, 181
Green, S., Montgomery, J. A., & Thaddeus, P. 1974, ApJ, 193, L89
Green, S., & Thaddeus, P. 1974, ApJ, 191, 653
Green, S., & Thaddeus, P. 1976, ApJ, 205, 766
Grosjean, A., Dubernet, M.-L., & Ceccarelli, C. 2003, A&A, 408, 1197
Gudeman, C. S., & Woods, R. C. 1982, Phys. Rev. Lett., 48, 1344
Hocking, W. H., Gerry, M. C. L., & Winnewisser, G. 1975, Can. J. Phys., 53, 1869
Hoeft, J., Lovas, F. J., Tiemann, E., & Törring, T. 1969, Z. Naturforsch., 24a, 1422
Hogerheijde, M. R., & van der Tak, F. F. S. 2000, A&A, 362, 697
Hutson, J. M., & Green, S. 1994, MOLSCAT User manual, http://www.giss.nasa.gov/molscat
Jankowski, P., & Szalewicz, J. 1998, J. Chem. Phys., 108, 3554
Jansen, D. J. 1995, Ph.D. Thesis, Leiden University
Jansen, D. J., van Dishoeck, E. F., & Black, J. H. 1994, A&A, 282, 605
Jaquet, R., Staemmler, V., Smith, M., & Flower, D. 1992, J. Phys. B, 25, 285
Johnson, C. T., Burke, P. G., & Kingston, A. E. 1987, J. Phys. B, 20, 2553
Juvela, M. 1997, A&A, 322, 943
Kochanski, E., & Flower, D. R. 1981, Chem. Phys., 57, 217
Larsson, B., Liseau, R., & Men'shchikov, A. B. 2002, A&A, 386, 1055
Launay, J. M., & Roueff, E. 1977, J. Phys. B, 10, 879
Lindqvist, M., Schöier, F. L., Lucas, R., & Olofsson, H. 2000, A&A, 361, 1036
Lovas, F. J., Suenram, R. D., Ogata, T., & Yamamoto, S. 1992, ApJ, 399, 325
Müller, H. S. P., Thorwirth, S., Roth, D. A., & Winnewisser, G. 2001, A&A, 370, L49
Mangum, J. G., & Wootten, A. 1993, ApJS, 89, 123
Manolopoulos, D. E. 1986, J. Chem. Phys., 85, 6425
Maret, S., Ceccarelli, C., Caux, E., et al. 2004, A&A, 416, 577
Mengel, M., & De Lucia, F. C. 2000, ApJ, 543, 271
Mengel, M., Flatin, D., & De Lucia, F. 2000, J. Chem. Phys., 112, 4069
Monteiro, T. 1984, MNRAS, 210, 1
Monteiro, T. S., & Stutzki, J. 1986, MNRAS, 221, 33
Muenter, J. S. 1968, J. Chem. Phys., 48, 4544
Neufeld, D. A., & Green, S. 1994, ApJ, 432, 158
Offer, A. R., & van Dishoeck, E. F. 1992, MNRAS, 257, 377
Offer, A. R., & van Hemert, M. C. 1993, J. Chem. Phys., 99, 3836
Offer, A. R., van Hemert, M. C., & van Dishoeck, E. F. 1994, J. Chem. Phys., 100, 362
Ossenkopf, V., Trojan, C., & Stutzki, J. 2001, A&A, 378, 608
Patel, D., Margolese, D., & Dyke, T. R. 1979, J. Chem. Phys., 70, 2740
Peterson, K. I., Fraser, G. T., & Klemperer, W. A. 1984, Can. J. Phys., 62, 1502
Phillips, T. G., van Dishoeck, E. F., & Keene, J. 1992, ApJ, 399, 533
Phillips, T. R., Maluendes, S., & Green, S. 1996, ApJS, 107, 467
Pickett, H. M., Poynter, R. L., Cohen, E. A., et al. 1998, J. Quant. Spec. Rad. Transfer, 60, 883
Pottage, J. T., Flower, D. R., & Davis, S. L. 2001, J. Phys. B, 34, 3313
Pottage, J. T., Flower, D. R., & Davis, S. L. 2002, J. Phys. B, 35, 2541
Pottage, J. T., Flower, D. R., & Davis, S. L. 2004, MNRAS, submitted
Raymonda, J. W., Muenter, J. S., & Klemperer, W. A. 1970, J. Chem. Phys., 52, 3458
Rothman, L. S., Barbe, A., Chris Benner, D., et al. 2003, J. Quant. Spec. Rad. Transfer, 82, 5
Roueff, E. 1990, in Molecular Astrophysics, ed. T. W. Hartquist (Cambridge University Press), 232
Roueff, E., Dubernet, M. L., Flower, D. R., & Pottage, J. T. 2004, in The Dense Interstellar Medium in Galaxies, 413
Roueff, E., & Le Bourlot, J. 1990, A&A, 236, 515
Sastry, K. V. L. N., Lees, R. M., & Van der Linde, J. 1981, J. Mol. Spec., 88, 228
Schöier, F. L., Jørgensen, J. K., van Dishoeck, E. F., & Blake, G. A. 2002, A&A, 390, 1001
Schöier, F. L., & Olofsson, H. 2001, A&A, 368, 969
Schinke, R., Engel, V., Buck, U., Meyer, H., & Diercksen, G. H. F. 1985, ApJ, 299, 939
Schmid-Burgk, J., Muders, D., Müller, H. S. P., & Brupbacher-Gatehouse, B. 2004, A&A, 419, 949

Schreel, K., & ter Meulen, J. J. 1996, J. Chem. Phys., 105, 4522
Schröder, K., Staemmler, V., Smith, M. D., Flower, D. R., & Jacquet, R. 1991, J. Phys. B, 24, 2487
Staemmler, V., & Flower, D. R. 1991, J. Phys. B, 24, 2343
Stutzki, J., & Winnewisser, G. 1985, A&A, 144, 1
Suenram, R. D., Lovas, F. J., & Matsumura, K. 1989, ApJ, 342, L103
Townes, C. H., & Schawlow, A. L. 1975, Microwave Spectroscopy (New York: Dover)
Truong-Bach, & Nguyen-Q-Rieu. 1989, A&A, 214, 267
Turner, B. E., Chan, K., Green, S., & Lubowich, D. A. 1992, ApJ, 399, 114
van der Tak, F. F. S., Boonman, A. M. S., Braakman, R., & van Dishoeck, E. F. 2003, A&A, 412, 133
van Dishoeck, E. F., & Hogerheijde, M. R. 1999, in NATO ASIC Proc. 540: The Origin of Stars and Planetary Systems, 97
van Zadelhoff, G.-J., Dullemond, C. P., van der Tak, F. F. S., et al. 2002, A&A, 395, 373
Wilson, N. J., & Bell, K. L. 2002, MNRAS, 337, 1027
Winnewisser, G., & Cook, R. L. 1968, J. Mol. Spec., 28, 266
Woods, R. C., Saykally, R. J., Dixon, T. A., & Szanto, P. G. 1975, Phys. Rev. Lett., 35, 1269
Ziurys, L. M., & Apponi, A. J. 1995, ApJ, 455, L73
Ziurys, L. M., & Turner, B. E. 1986, ApJ, 300, L19

Online Material

6. Extrapolation of collisional rate coefficients

6.1. Linear molecules

An often adopted starting point when fitting and extrapolating collisional rate coefficients is to take advantage of the IOS approximation in which the entire matrix of state-to-state rate coefficients can be calculated from the basic γ_{L0} rate coefficients (e.g. Goldflam et al. 1977)

$$\gamma_{JJ'} = (2J'+1)\sum_{L=|J-J'|}^{J+J'}(2L+1)\begin{pmatrix} J & J' & L \\ 0 & 0 & 0 \end{pmatrix}^2 \gamma_{L0}, \quad (14)$$

where

$$\begin{pmatrix} J & J' & L \\ 0 & 0 & 0 \end{pmatrix} \quad (15)$$

is the Wigner 3-j symbol. This expression is valid only in the limit where the kinetic energy of the colliding molecules is large compared to the energy splitting of the rotational levels. Since the energy splitting increases with J this expression becomes less accurate for higher rotational levels. DePristo et al. (1979) show that by multiplying Eq. (14) (within the summation) with

$$A(L,J) = \frac{6+\Omega(L)^2}{6+\Omega(J)^2}, \quad (16)$$

where

$$\Omega(J') = 0.13\, J' B_0\, l \left(\frac{\mu}{T}\right)^{1/2}, \quad (17)$$

one can approximately correct for this deficiency. Here B_0 is the rotational constant in cm^{-1}, l is the scattering length in Å (typically $l \approx 3$ Å), μ is the reduced mass of the system in amu and T is the kinetic temperature in K. Extrapolation of the rate coefficients down to the lowest $J = 0$ level can be made both in temperature as well as in J allowing the general state-to-state coefficients to be extended (e.g., Albrecht 1983; Larsson et al. 2002).

Alternatively, and in line with the IOS approximation, the downward collisional rate coefficients ($\Delta J = J_u \rightarrow J_l$, $J_u > J_l$) can be extrapolated in temperature using Eq. (13). Given its simplicity we have adopted this procedure for extrapolation of the rate coefficients in temperature.

Extrapolation to include higher rotational levels was carried out by fitting the collisional rate coefficients connecting to the ground rotational state, at a particular temperature, to a second order polynomial

$$\gamma_{J0} = \exp(a + bJ + cJ^2), \quad (18)$$

where a, b and c are parameters determined from the fit. Figure 3 illustrates the fit to collisional rate coefficients down to the ground rotational state for CO–H_2 using Eq. (18). Similar extrapolations can be made in temperature. However, here we have adopted the approach by de Jong et al. (1975) and Bieging et al. (1998) and used Eq. (13) for the extrapolation in temperature. This extends the fit over a larger range of energies. The IOS approximation (Eq. (14)) was then used to calculate the entire matrix of state-to-state rate coefficients. The CO molecule is used in Sect. 4.3.1 to illustrate the above mentioned schemes.

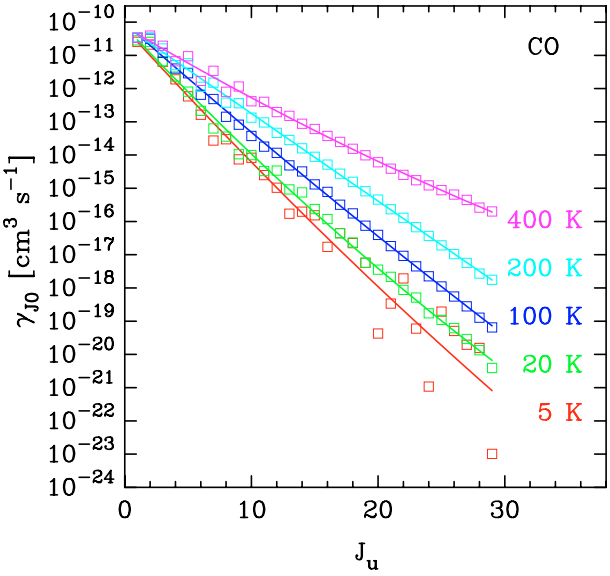

Fig. 3. The solid lines are fits to the CO–p-H_2 collisional rate coefficients from Flower (2001a) (squares) for transitions down to the ground state from upper energy levels J_u using a second order polynomial.

6.2. Non-linear molecules

For non-linear species there are no simple scaling relations and one has to resort to custom-made fitting formulae for each case. The only case considered here is that of SO_2 used by van der Tak et al. (2003). In the prolongation of this project extrapolated collisional rate coefficients will be presented for additional non-linear molecules. As the starting point for inelastic collisional data for SO_2, the results of Green (1995) were used. However, those data only cover the lowest 50 states, up to 62 cm^{-1} ($J \approx 12$), while states up to $J = 25$ are commonly observed.

Figure 4 plots Green's downward rate coefficients, summed over all final states, as functions of initial state. These sums approach asymptotic values for $E_u \gtrsim 40$ cm^{-1}. Deviations from this behaviour due to detailed quantum mechanical selection rules are seen not to exceed 20%. The figure also shows that the rate coefficients increase approximately as $T^{1/2}$, again to ≈20% accuracy. This behaviour indicates that the total rate coefficients only depend on temperature through the collision velocity, while the de-excitation cross sections are constant.

Figure 5 shows that most collisions lead to de-excitation into states that are not far down in energy. The thick black curve is our fit to this behaviour: it is the normalized mean of the various thin light curves which represent Green's data. Transitions by more than 15 states are considered negligible.

Based on these trends, the rate coefficients for de-excitation of SO_2 in inelastic collisions with He are extrapolated as follows. For the 50 lowest states, Green's values at $25 < T < 125$ K are used and multiplied by $(T/125\,\mathrm{K})^{1/2}$ at temperatures up to 375 K and down to 10 K. For states between 62 and 250 cm^{-1} above ground, a total de-excitation rate coefficient of $1.0 \times 10^{-11}\ T^{1/2}$ cm^{-3} s^{-1} is assumed, shown by Fig. 4 to be a good zeroth-order description for other levels. The state-to-state rate coefficients are derived by multiplying these totals by

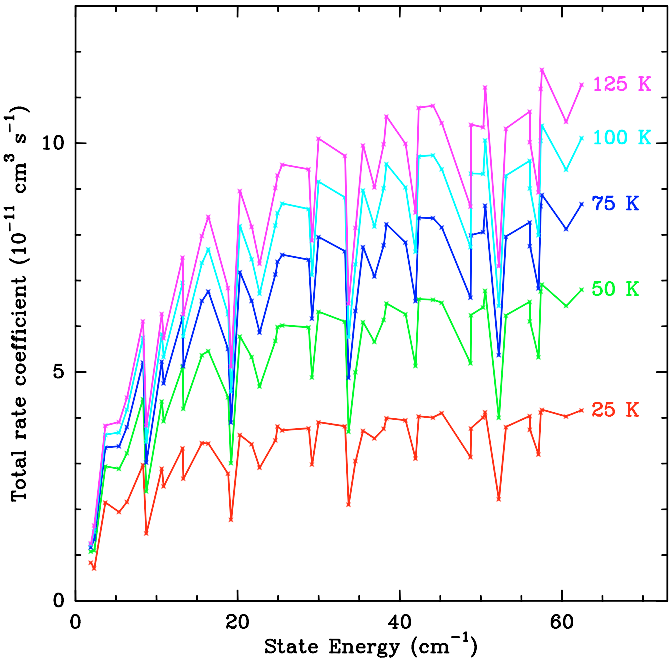

Fig. 4. Collisional de-excitation rate coefficients for the lowest 50 states of SO_2 summed over all lower levels, calculated from the data by Green (1995) for various temperatures.

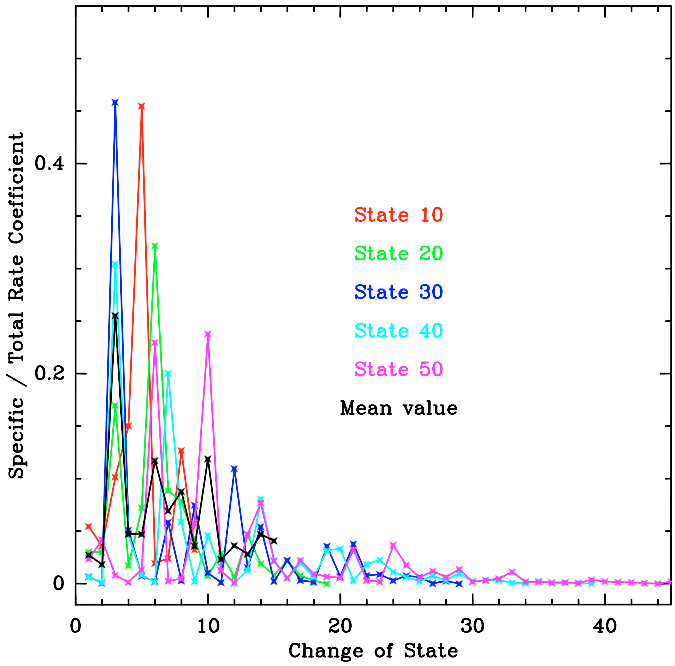

Fig. 5. State-to-state de-excitation rate coefficients for SO_2 as fractions of the total downward rate coefficient (Fig. 4), as a function of the number of levels by which the transition is changed. The light (coloured) curves are values from Green (1995) at $T = 25$ K for the 10th, 20th, 30th, 40th and 50th state above ground. The thick black curve is the normalized mean of the light (coloured) curves, adopted here to extrapolate Green's rate coefficients to higher-lying levels. The states are labelled in order of increasing energy.

the mean propensities from Green (1995), given by the black curve in Fig. 5. All results are multiplied by 1.4 to account for the mass difference between H_2 and He. While this procedure is admittedly crude and does not take the detailed quantum mechanics of the interaction into account, it catches the spirit of more detailed calculations.